IEEE Access
Multidisciplinary | Rapid Review | Open Access Journal

Date of publication xxxx 00, 0000, date of current version xxxx 00, 0000.

Digital Object Identifier 10.1109/ACCESS.2017.DOI

Efficient Template Cluster Generation for Real-Time Abnormal Beat Detection in Lightweight Embedded ECG Acquisition Devices

SEUNGMIN LEE[1], (Associate Member, IEEE), DAEJIN PARK[1,2],(MEMBER, IEEE)
[1]School of Electronic and Electrical Engineering, Kyungpook National University, DAEGU 41566 KOREA (e-mail: lsm1106@knu.ac.kr; boltanut@knu.ac.kr)
[2]School of Electronics Engineering, Kyungpook National University, DAEGU 41566 KOREA

Corresponding author: Daejin Park(e-mail: boltanut@knu.ac.kr).

This work was partly supported by Institute of Information & communications Technology Planning & Evaluation (IITP) grant funded by the Korea government(MSIT) (No. 2021-0-00944, Metamorphic approach of unstructured validation/verification for analyzing binary code), the BK21 Project funded by the Ministry of Education (4199990113966), and Basic Science Research Program through the National Research Foundation of Korea(NRF) funded by the Ministry of Education (NRF-2020R1I1A1A01072343, NRF-2018R1A6A1A03025109) and the Ministry of Science and ICT (NRF-2019R1A2C2005099).

ABSTRACT

Recently, as interest in electrocardiogram monitoring has increased, research on real-time ECG signal analysis in daily life using lightweight embedded devices has increased. Abnormal beat detections in ECG signal analysis are an important research area to reduce processing time and cost for cardiac arrhythmia diagnosis. Abnormal beat detections can be divided into feature-based detection and shape-based detection. Feature-based detection finds it difficult to detect reliable fiducial points, and shape-based detection has difficulty detecting abnormal beats that are similar to normal beats. In this paper, we propose template cluster generation and abnormal beat detection using both detection methods. The proposed method shows robust detection of distorted normal beats by generating a template cluster rather than a single template. Moreover, abnormal beats that have normal shape can be detected using the RR interval, which is a highly reliable feature. Experiment results using the MIT-BIH arrhythmia database, provided by Physionet, showed the average processing times to generate a template cluster and detect abnormal beats for the 30-minute signal length were 1.21 seconds and 0.14 seconds, respectively. With manually adjusted thresholds, the specificity and accuracy achieved 93.00% and 97.94%, respectively. In the case of group 1 records obtained relatively stably, the specificity and accuracy achieved 99.27% and 99.44%.

INDEX TERMS Electrocardiogram, embedded system, template cluster, RR interval, abnormal beat detection

I. INTRODUCTION

Recently, average life expectancy has been prolonged with the development of medical technology. With an increasing older population, the percentage of deaths due to heart disease increases. Thus, research on early detection and monitoring of heart disease through electrocardiogram (ECG) signal analysis is of interest [1], [2]. Recent studies on the measurement and analysis of ECG signals using embedded devices are actively being conducted using lightweight wearable systems [3], [4]. In particular, a real-time signal processing technique in a low-power and low-memory environment is required [5], [6]. In addition, in the case of the ECG monitoring system, the beat detection and abnormal beat classification in real-time are important. The beat can be reliably detected using Pan's method [7]. In the case of abnormal beat detection, detection methods can be roughly divided into feature-based detection using the fiducial points [8]–[11] and shape-based detection using the shape of a beat, centered on R-peak [12]–[14].

In general, the normal beats have similar features or shape because beats with a similar shape periodically repeated. On the other hand, the abnormal beats have features outside the

This article has been accepted for publication in a future issue of this journal, but has not been fully edited. Content may change prior to final publication. Citation information: DOI 10.1109/ACCESS.2021.3077628, IEEE Access

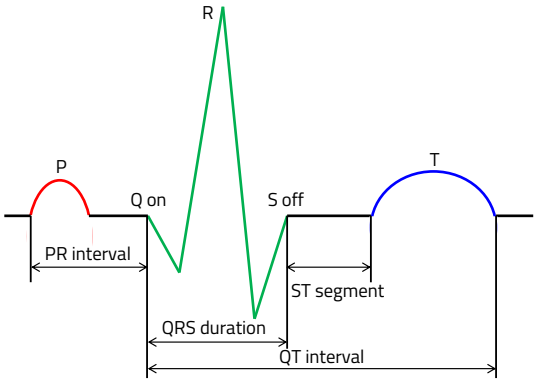

FIGURE 1. The fiducial points and features of an ECG signal.

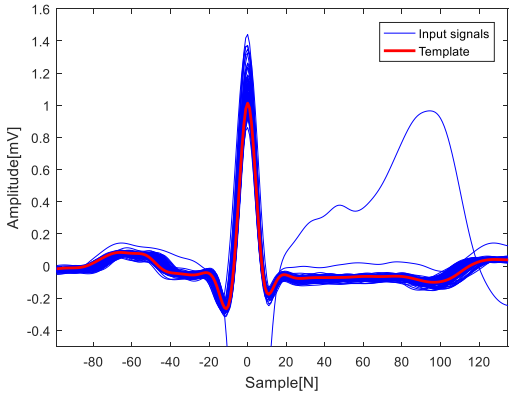

FIGURE 2. Example of signal cluster and template.

normal distribution or low shape similarity to normal beats. The abnormal beat detection proceeds based on these characteristics. Feature-based detection is based on the detection of fiducial points such as the onset, peak, and offset of each waveforms. Then, the feature values of fiducial points, such as intervals, segments, and amplitudes, are used to detect abnormal beats. Fig. 1 shows the generally used fiducial points and feature values in feature-based abnormal beat detection.

The beats are divided around the QRS complex because they are generated in the order of P-wave, QRS complex, and T-wave [15]. In particular, the R-peak has the highest amplitude, so it is easy to detect and generally used to separate beats. Pan's method is a typical QRS detection method and has high detection accuracy.

In abnormal beat detection, premature ventricular contraction (PVC) and premature atrial contraction (PAC), which have the highest frequencies, can be detected using the RR interval and the amplitude of R-peak. R-peak has local extreme amplitude. Reliable R-peak detection is possible by calibrating to local extrema point. However, the onset and offset of QRS complex and P-wave are hard to calibrate because these fiducial points are ambiguous rather than R-peak. Therefore, an error occurs in detection of the fiducial points [16], [17], and the error of feature value is more large because the feature value uses the interval between the fiducial points. These make it difficult to detect an abnormal beat based on feature values.

Shape-based detection generates a template to store shape information on a normal beat and measure similarity with the generated template to detect an abnormal beat.

Fig. 2 shows the cluster of input signals and the template.

The detection is easy and reliable based on the shape deformation caused by the abnormal beat. However, shape-based detection requires a manually determined template or it requires a great deal of memory to determine the template from the input signals.

Fig. 3 summarizes the weakness of the existing template generating methods and the techniques proposed in this paper for improvement.

As shown in Fig. 3, the manual template determination method has to be applied each signal because the shape of the beat varies depending on the individual. As a method for automatically determining a template, there is a method using a mean and a median of input beats [18]. However, when a mean is used in template generation, a distorted template might be acquired due to an abnormal beat. If the median is used in template generation, then distortion caused by abnormal beats can be minimized based on the characteristic in which the normal beats are the majority in the general ECG signals. However, it is not suitable for embedded devices because all input beats must be stored in memory. In addition, the technique is vulnerable to the detection of abnormal beats that have no shape deformation, such as PACs. PACs can be detected using the RR interval deformation. The proposed method solves these problems through the template-cluster generation.

In this paper, we propose a template-based abnormal beat detection method in a real-time lightweight embedded device. The proposed method uses feature-based detection using RR interval and shape-based detection using template.

Feature-based detection using the RR interval can detect PVCs and PACs. However, in the case of a fusion beat in which ventricular and normal beat are mixed, it cannot be detected because the RR interval is similar to normal. Shape-based detection can detect PVCs and fusion beats, but cannot detect PACs because their shape is similar to normal. Therefore, a template applied with RR interval and shape is generated to detect PVCs, PACs, and fusion beats. The similarity used in the process of generating the template and detecting abnormal beats is based on the similarity of RR intervals and the shape of the waveform. The similarity of the RR intervals uses the ratio, and the shape similarity uses the Pearson similarity. We propose a template cluster rather than a single template to improve the problem caused by misidentification of normal beats with slight shape deformations as abnormal beats. In addition, an independent template-cluster update process for each beat minimizes memory usage and processing time. Then, the cluster is optimized

This article has been accepted for publication in a future issue of this journal, but has not been fully edited. Content may change prior to final publication. Citation information: DOI 10.1109/ACCESS.2021.3077628, IEEE Access

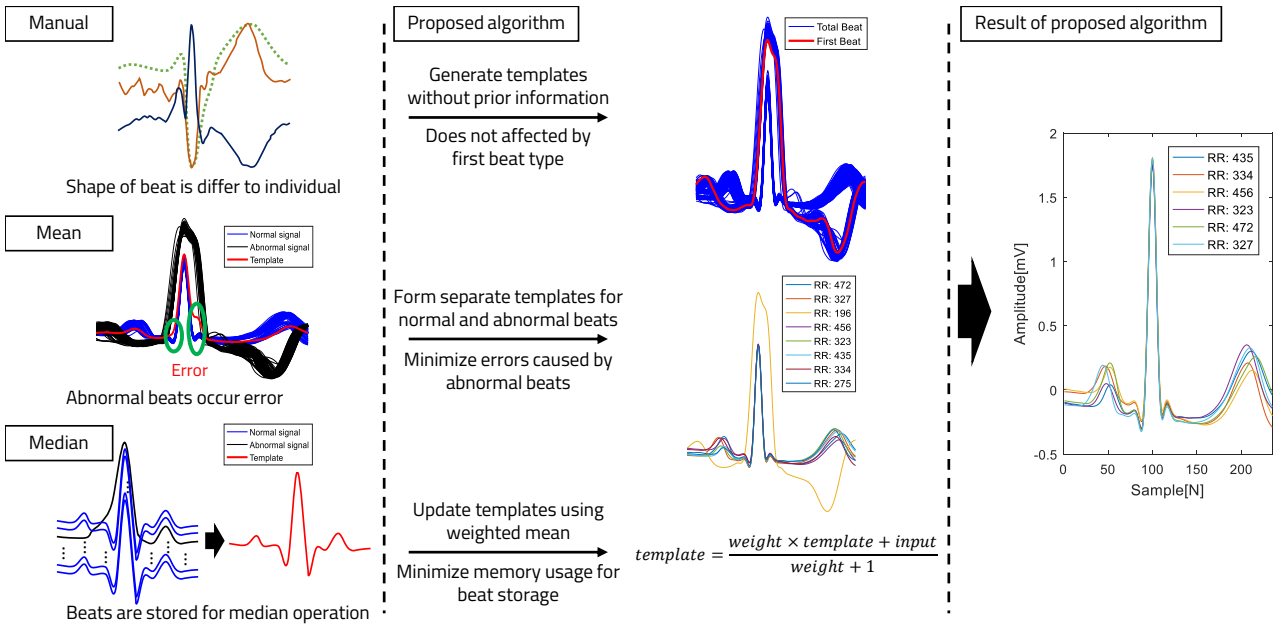

FIGURE 3. Summary of existing methods and proposed method.

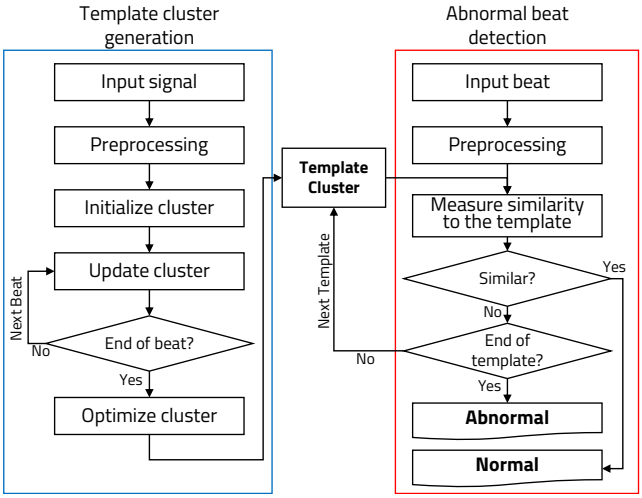

FIGURE 4. Algorithm flowchart.

by removing unnecessary templates from it, and templates are sorted according to importance. After generating the template cluster, an input beat is sequentially compared with the sorted templates, and it is determined to be normal if a similar template exists. In the most case of the normal beat, it is determined as the normal beat through the similarity to the first template with the highest importance. Thus, time complexity of abnormal detection can be reduced.

Fig. 4 shows the algorithm flow of the proposed method.

The composition of paper is as follows. In Section 2, the characteristics of abnormal beats in the ECG signal are analyzed. In Section 3, the pre-processing, R-peak detection, and Pearson similarity are introduced, and then the proposed algorithm is described in Section 4. Section 5 shows the experiment results in MIT-BIH arrhythmia database (MIT-BIH ADB) [19] and Section 6 concludes the paper.

II. ABNORMAL BEATS IN ECG SIGNAL

ECG signals show various types of abnormal beats. ANSI-AAMI EC57: 1998 of the American Medical Association categorizes into five categories that include normal beat (N), upper ventricular arrhythmia beat (S), ventricular arrhythmia beat (V), mixed arrhythmia beat (F), and unclassified beat (Q) [20], [21].

Physionet provides 19 categories of MIT-BIH ADB as a method of subdividing the type of beat, which is a widely used method. Table 1 shows the distribution of 19 type categories of 48 records in MIT-BIH ADB.

In this paper, we detect V, A, and F type abnormal beats with high frequency.

Fig. 5 shows examples of abnormal beats.

Fig. 5(a) is an example of a PVC called type V. The RR interval becomes shorter, and shape deformation occurs. Fig. 5(b) is an example of a PAC called type A. The RR interval becomes shorter, but the shape is similar to normal. Fig. 5(c) is a deformed V-type beat called type F. The shape deformation occurs, but the RR interval is similar to normal.

Based on these characteristics, when detecting only the V-type abnormal beat, both feature-based detection and shape-based detection are effective. However, type A is difficult to detect using shape-based detection. On the other hand, type F is difficult to detect using a feature-based detection.

To solve this diversity of abnormal beats, this paper proposes an effective detection method by mixing feature-based detection and shape-based detection.

This article has been accepted for publication in a future issue of this journal, but has not been fully edited. Content may change prior to final publication. Citation information: DOI 10.1109/ACCESS.2021.3077628, IEEE Access

TABLE 1. Distribution of beats in MIT-BIH ADB.

Code	Total number	Description	Class
N	75052	Normal beat	Normal
L	8075	Left bundle branch block beat	Bundle branch block
R	7259	Right bundle branch block beat	
B	0	Bundle branch block beat	
A	**2546**	Atrial premature beat	Premature
a	150	Aberrated atrial premature beat	
J	83	Junctional premature beat	
S	2	Supraventricular premature beat	
V	**7130**	Premature ventricular contraction	
r	0	R-on-T premature ventricular contraction	
F	**803**	Fusion of ventricular and normal beat	
e	16	Atrial escape beat	Escape
j	229	Junctional escape beat	
n	0	Supraventricular escape beat	
E	106	Ventricular escape beat	
/	7028	Paced beat	Paced
f	982	Fusion of paced and normal beat	
Q	33	Unclassifiable beat	Else
?	0	Beat not Classified during learning	

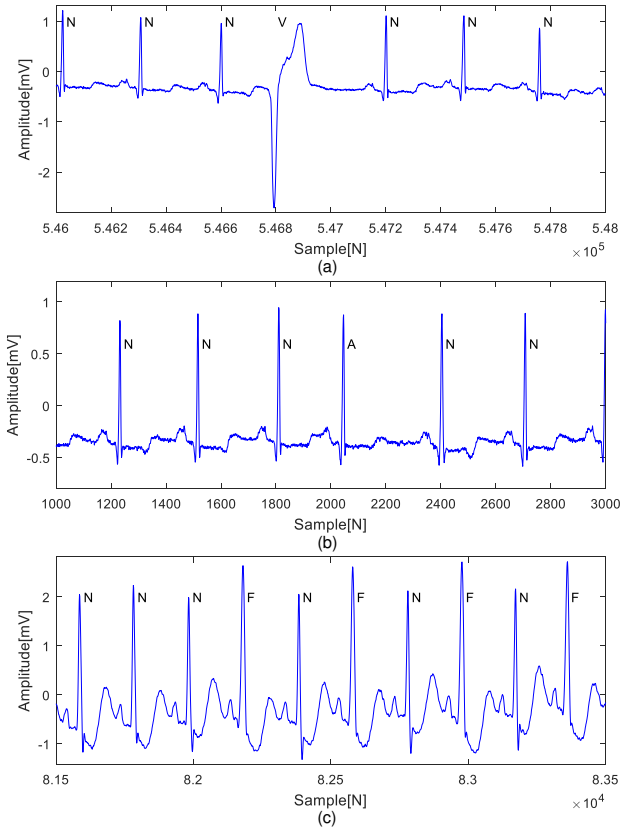

FIGURE 5. Examples of abnormal beats: (a) V, (b) A, (c) F.

III. MATERIALS AND METHODS

A. PREPROCESSING

In ECG signals, various noises are mixed in the measurement process because the ECG is an electrical signal generated from the activity of the heart [22]–[24]. Typical noise is as follows: 1) power line interference, 2) baseline movement, 3) miscellaneous noise.

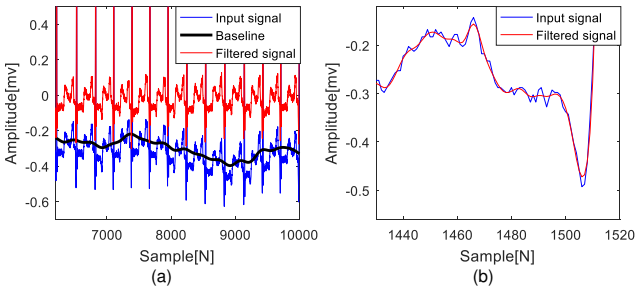

FIGURE 6. Examples of ECG signal noise suppression: (a) the suppression of baseline movements, (b) the suppression of high frequency noises.

The power line interference noise appears as high frequency noise of 30 Hz or higher. In 46 records of MIT-BIH ADB used in this paper, 19 records have 30 Hz noise and 27 records have 60 Hz noise. Baseline movement caused by breathing appears as low frequency noise of 0.1 Hz or lower. Therefore, preprocessing using a band-pass filter is generally used, and in this paper, a 1-25 Hz third-order Butterworth band-pass filter was used to suppress noises.

Fig. 6 shows the input signal including low- and high-frequency noises and the filtered result.

B. PAN'S METHOD

In the ECG signal, R-peak generally has the highest amplitude among the fiducial points. Most ECG signal analysis is performed based on the detection of the R-peak because R-peak is relatively easy to detect compared to other fiducial points. Various methods exist for the detection of R-peak, of which Pan's method is the most representative.

The signal is variously filtered using band-pass filter, differential filter, average filter, etc., and a QRS complex is detected using an adaptively determined threshold according to these filtered signals. This method has an excellent ability to detect a 99.3% QRS complex for 24 hours of MIT-BIH ADB signal, so it is used as a preprocess for R-peak detection in various ECG signal analyses.

C. RR INTERVAL RATIO

The obtained R-peak is not only used as a reference for acquiring the waveform shape, but also the RR interval from the previous R-peak to the present R-peak can be used as an important feature value. In general, a normal beat has a constant R-peak interval. However, when an abnormal beat occurs, deformation occurs in the RR interval, and premature contraction generally shortens the RR interval. Therefore, when measuring the ratio (RR_{Ratio}) of the RR interval of a normal beat (RR_N) and abnormal beat (RR_A) as shown in (1), the ratio is less than 1, and generally, it is less than 0.9.

$$RR_{Ratio} = \frac{RR_A}{RR_N} \tag{1}$$

A normal beat that occurs after an abnormal beat has a characteristic in which the RR interval is longer than normal

This article has been accepted for publication in a future issue of this journal, but has not been fully edited. Content may change prior to final publication. Citation information: DOI 10.1109/ACCESS.2021.3077628, IEEE Access

due to the compensatory pause. In this case, the RR interval ratio has a value lager than 1, and it is modified to have a smaller value compared to 1 as shown in (2) so that it is similar to the RR interval ratio of other normal beats.

$$RR_{Ratio} = \min\left(1, \frac{RR_A}{RR_N}\right) \tag{2}$$

Based on this, the RR interval of the abnormal beat can be emphasized and easier to detect. However, in the case of an abnormal beat that occurs continuously more than 3 times at a time, the RR interval ratio of the internal section is close to 1, so the internal abnormal beats are detected as normal beats. To solve this problem, a reclassification process for the internal section is required, but it makes real-time processing difficult. Thus, the RR interval is used instead of the RR interval ratio in this paper.

D. PEARSON SIMILARITY

To measure the similarity between the template and the input signal, the Pearson similarity is used in this paper. The Pearson similarity is well known in statistics as the Pearson correlation coefficient, which is a value quantified for linear distributions for two distributions X and Y, with a value between 1 and –1. The value indicates perfect positive linear correlation at 1, no linear correlation at 0, and perfect negative linear correlation at –1. The Pearson similarity is the value obtained by the covariance of two distributions X and Y, which is divided by the product of the standard deviations as shown in (3).

$$\rho(X,Y) = \frac{1}{N-1}\sum_{i=1}^{N}\left(\frac{X-\mu_X}{\sigma_X}\frac{Y-\mu_Y}{\sigma_Y}\right) \tag{3}$$

As shown in (3), by subtracting the mean and dividing by the standard deviation, the Pearson similarity is robust to baseline movements and amplitude scale changes. Thus, it is suitable for measuring the similarity of ECG signals.

IV. PROPOSED ALGORITHM

The proposed algorithm uses feature values and shape. If both are normal, then a beat is classed as normal; otherwise, it is classed as abnormal. Unlike the existing method in which a single template of a normal beat is used, this paper suggests a template-cluster generation method that considers the slight change in the normal beat or the distortion of feature values caused by a neighboring abnormal beat. Accordingly, the proposed algorithm is divided into 3 steps to generate the template cluster: 1) initialize the template cluster, 2) update the template cluster, and 3) optimize the template cluster.

A. INITIALIZATION

In this paper, the template is composed of three data points that consists of shape, RR interval, and a counting number of the template. From the first input signal, the shape and RR interval of the first beat are input as the first data point of the first cluster of templates, and the counting number of the first template is initialized to 1. The counting number indicates the weight of the weighted mean in the template update process and it is used to gauge the importance of the template in the template sorting process.

Alg. 1 shows the pseudo-code for the initialization process of the template cluster.

Algorithm 1: Template cluster initialization.

S^i : i_{th} input beat
RR^i : RR interval of i_{th} input beat
C_T^j : j_{th} template of cluster
C_{RR}^j : RR interval of j_{th} template
C_C^j : count of j_{th} template
N : number of template in cluster

% Initialization

$C_T^1 = S^1$
$C_{RR}^1 = RR^1$
$C_C^1 = 1$
$N = 1$

B. UPDATE

After entering the initial template, clusters are updated from the sequentially input beats. The input beats measure the RR interval ratio and shape similarity with each template in the template cluster using (2) and (3), respectively. Then, a template with the highest shape similarity among templates satisfying the threshold value of the RR interval ratio is detected. At this time, if shape similarity exceeds the threshold, then the matched template is updated, otherwise, the input beat is added as a new template.

The weighted mean of the RR interval and shape is used to update the template. The counting number of j_{th} template (C_C^j) is used as the weight of the weighted mean as shown in (4) and (5).

$$C_T^j(k) = \frac{C_C^j \times C_T^j(k) + S^i(k)}{C_C^j + 1} \tag{4}$$

$$C_{RR}^j = \frac{C_C^j \times C_{RR}^j + RR^i}{C_C^j + 1} \tag{5}$$

where $C_T^j(k)$ and $S^i(k)$ indicate the k_{th} samples of the j_{th} template and i_{th} input beat, respectively. In this way, the processed beat information can be deleted to minimize memory usage because the template cluster is sequentially updated for each beat.

Alg. 2 shows the pseudo-code for the updating process of the template cluster.

C. OPTIMIZATION

The updated template cluster not only has normal beat templates, but also various abnormal beat templates. Therefore,

This article has been accepted for publication in a future issue of this journal, but has not been fully edited. Content may change prior to final publication. Citation information: DOI 10.1109/ACCESS.2021.3077628, IEEE Access

Algorithm 2: Template cluster update.

M : maximum similarity
p : template number at M
RR_R : ratio of RR interval
P_S : Pearson similarity
T_{RR}^U : RR interval ratio threshold for update
T_P^U : Pearson similarity threshold for update

% Update

$M = 0, p = 1$ % Initialize
foreach *j from 1 to N* **do**
    Calculate RR_R and P_S between S^i and C_T^j
    if $RR_R > T_{RR}^U$ & $P_S > M$ **then**
        $M = P_S$
        $p = j$
if $M > T_P^U$ **then**
    % Update by using weighted mean
    $C_T^p = (C_C^p \times C_T^p + S^i)/(C_C^p + 1)$
    $C_{RR}^p = (C_C^p \times C_{RR}^p + S^i)/(C_C^p + 1)$
    $C_C^p = C_C^p + 1$
else
    % Add as a new template
    $N = N + 1$
    $C_T^N = S^i$
    $C_{RR}^N = RR^i$
    $C_C^N = 1$

removing the abnormal beat templates is necessary. In general, normal beats occupy the majority of the signals, and the template with the highest counting number is likely to be a representative template of a normal beat. Thus, after determining the template with the highest counting number as the representative template, the template with similarity to the representative template below the threshold is classed as the abnormal beat template and removed from the template cluster. Next, the template is sorted according to the counting number of each template, which makes it possible to classify a normal beat quickly using the abnormal beat detection step, thereby saving processing time.

Alg. 3 shows the pseudo-code for the optimization process of the template cluster.

Fig. 7 shows the sequential results of applying the proposed algorithm to Datum 119 of MIT-BIH ADB.

As shown in Fig. 7, even if the abnormal beat is selected as the initial beat, only the templates of the normal beat comprise the cluster through the update and optimization process.

D. ABNORMAL BEAT DETECTION

By using the template cluster, beats are classed as normal if there is a similar template and abnormal if not. Fig. 8 is the result of detecting normal and abnormal beats using the template cluster in Fig. 7(c).

Algorithm 3: Template cluster optimization.

mp : position of maximum in C_C
T_{RR}^O : RR interval ratio threshold for optimization
T_P^O : Pearson similarity threshold for optimization

% Optimization

foreach *j from 1 to* C_N **do**
    Calculate RR_R and P_S between C_T^{mp} and C_T^j
    if $RR_R < T_{RR}^O$ & $P_S < T_P^O$ **then**
        Remove j_{th} template
Sort templates according to C_C

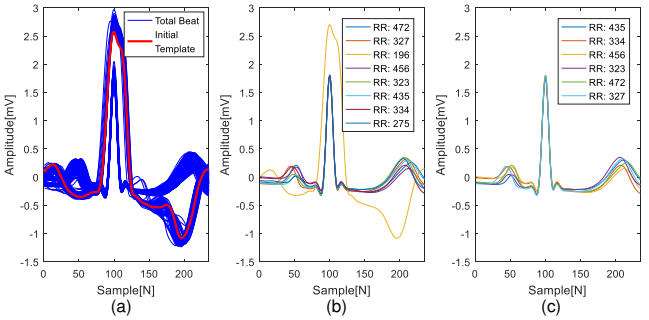

FIGURE 7. Examples of template cluster generation: (a) total beat and initial template, (b) updated template cluster, (c) optimized template cluster.

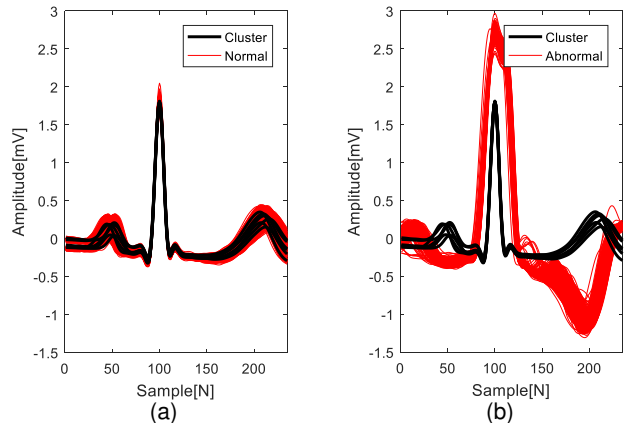

FIGURE 8. Examples of abnormal beat detection results of Fig. 7: (a) normal beats, (b) abnormal beats.

V. EXPERIMENTS

We conducted experiments to confirm the performance of the proposed algorithm. The template cluster and abnormal beat detection were generated for each MIT-BIH ADB record Physionet provided. The experimental environment of MIT-BIH ADB was Windows 10 64-bit OS, Intel i7-7700 3.60 GHz CPU, and MATLAB R2016.

TABLE 2. Classification of MIT-BIH ADB annotation.

Group 1 Record	Normal	Abnormal			Group 2 Record	Normal	Abnormal		
		V	A	F			V	A	F
100	2236	1	33	0	200	1741	825	30	2
101	1857	0	3	0	201	1622	198	30	2
102	2025	4	0	0	202	2058	19	36	1
103	2079	0	2	0	203	2526	444	0	1
104	1377	2	0	0	205	2568	71	3	11
105	2523	41	0	0	207	1457	104	106	0
106	1504	520	0	0	209	2618	1	383	0
107	2075	59	0	0	210	2420	194	0	10
108	1736	17	4	2	212	1823	0	0	0
109	2489	38	0	2	213	2638	220	25	362
111	2120	1	0	0	214	2000	256	0	1
112	2534	0	2	0	215	3192	164	3	1
113	1786	0	0	0	217	1539	162	0	0
114	1817	43	10	4	219	2079	64	7	1
115	1950	0	0	0	220	1951	0	94	0
116	2299	109	1	0	221	2028	396	0	0
117	1531	0	1	0	222	2059	0	208	0
118	2163	16	96	0	223	2026	473	72	14
119	1541	443	0	0	228	1685	362	3	0
121	1858	1	1	0	230	2252	1	0	0
122	2473	0	0	0	231	1251	2	1	0
123	1512	3	0	0	233	2228	830	7	11
124	1528	47	2	5	234	2697	3	0	0
Total	45013	1345	155	13	Total	48458	4789	1008	417
					Overall total	93471	6134	1163	430

A. MIT-BIH ADB

Each MIT-BIH ADB record is 30 minutes long with high sampling frequency of 360 Hz, including arrhythmias. MIT-BIH ADB is widely used for the study of ECG signal analysis because the locations and types of beats are annotated.

In Table 1, 19 types of beat were introduced, but in this paper, experiments were conducted to detect V, A, and F type abnormal beats. In the case of left bundle branch, right bundle branch, and pacemaker beat, these beats were regarded as normal because they occurred instead of normal beats. Among the records, Datum 208 and Datum 232 were excluded from the experiment because of the proportions of abnormal beats were abnormally large (46% and 78%), which were difficult to apply to the proposed algorithm. Accordingly, the overall beat distribution of the data used in the experiment is shown in Table 2.

The Datum of 113, 122, and 212 were used to confirm the incidence of false detections from the normal beat to the abnormal beat, although there are no V, A, and F type abnormal beats.

B. EXPERIMENTS

1) Processing Time

The processing time can largely be divided into the template cluster generation step and the abnormal beat detection step. The processing time of each step increases according to the number of templates because the main process is the similarity calculation with each template in the template cluster.

The distribution of processing time for 46 records of MIT-BIH ADB is shown as Fig. 9.

In the template generating process, Datum 203 (which is the 27th record in the experiment) has the longest processing time of 10.23 seconds, which takes about 8.5 times the average processing time (1.21 seconds). This is because various types of beats appear due to unstable measurements, and 159 templates are generated after the cluster update process, resulting in a rapid increase in unnecessary comparison calculations. After removing the abnormal beat templates, the number of templates become 15. The processing time of abnormal beat detection of Datum 203 is also longest (0.62 seconds) because the number of templates is about 3.2 times more than the average number of templates (4.7 templates). However, considering that the input signal is thirty-minutes long, even for the data that took the longest time, it took only 10.23 seconds and 0.62 seconds for the template cluster generation and abnormal beat detection process, respectively. Thus, real-time learning and detection of the proposed algorithm is possible.

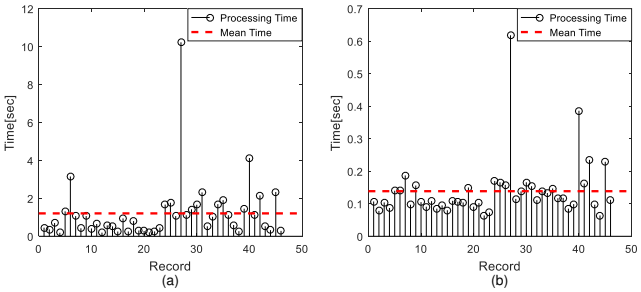

FIGURE 9. Processing times for 46 thirty-minute records in MIT-BIH ADB: (a) template cluster generation, (b) abnormal beat detection.

In the case of algorithm convergence, the number of templates in the update step is important as shown in Fig. 9. In extreme case, every beat forms an individual template, causing a problem that the execution time and memory usage increase exponentially. In general, since the normal beats of similar shape occupy most of the signals, in the experimental process of this paper, the process of generating a template cluster for the 30 minutes lengthy data only took about 10 seconds and 159 templates for the worst data. If it is implemented in an embedded device with limited memory, stable operation will be possible by converging the algorithm by limiting the number of templates and merging similar templates.

2) Detection performance

Confirming the performance of abnormal beat detection requires sensitivity (Se), specificity (Sp), and accuracy (Ac). Se, Sp, and Ac are expressed as (6).

$$\begin{aligned} Se &= \frac{TP}{TP+FN} \\ Sp &= \frac{TN}{TN+FP} \\ Ac &= \frac{TP+TN}{TP+TN+FP+FN} \end{aligned} \tag{6}$$

This article has been accepted for publication in a future issue of this journal, but has not been fully edited. Content may change prior to final publication. Citation information: DOI 10.1109/ACCESS.2021.3077628, IEEE Access

TP indicates true positive, which is the number of normal beats detected as normal beats, and TN indicates true negative, which is the number of abnormal beats detected as abnormal beats. FP indicates false positive, which is the number of abnormal beats detected as normal beats, and FN indicates false negative, which is the number of normal beats detected as abnormal beats. That is, the higher the Se, the fewer undetected beats; the higher the Sp, the fewer over-detected beats; and the higher the Ac, the better the overall performance. In addition, the overall performances are calculated by (6) after adding all the detected beats for each record because each record has different number of normal and abnormal beats as shown in Table 2.

Table 3 shows the overall detection performance with fixed threshold.

There is no clear detection in the same threshold and measurement environment because the feature value and shape of a normal beat are different for each individual, and the type of abnormal beat is different. Therefore, the thresholds should be determined individually for each record. In this paper, we change the thresholds according to the record, obtain the thresholds with the highest detection rate, and analyze the detection result at this time to confirm the possibility of the automated abnormal beat detection algorithm.

The results of learning and detection with manual thresholds for each individual are shown in Table 4.

It can be confirmed that the ratio of the existing undetected and over-detected beats was significantly reduced. Using the fixed threshold, Se, Sp, and Ac showed low detection rates of 93.96%, 80.35%, and 92.92%, respectively, but using the manually determined thresholds individually, they were greatly improved to 98.35%, 93.00%, and 97.94%. Therefore, we enable to detect abnormal beat through appropriate threshold determination with stably acquired ECG signal.

In particular, the proposed method is stable even for continuous abnormal beats input, because template cluster updates and abnormal beat detection are performed independently for the input beats. In the case of datum 124, 17 consecutive abnormal beats are input, but it can be confirmed that excellent abnormal beat detection is possible as shown in Table 4. In datum 124, the false detected two abnormal beats are the F-type and A-type abnormal beats, respectively. They are the exceptions that were erroneously detected because they are very similar to the normal beat.

However, there are still data with a high ratio of undetected and over-detected beats. This is a case where a large amount of over-detection occurs because the shape or interval information of the normal beat is significantly changed from a specific section as shown in Fig. 10.

Another cause is a large signal distortion even after preprocessing due to sudden baseline change as shown in Fig. 11.

Pearson similarity is robust to change of amplitude scale and average amplitude, but false detection occurs when baseline is inclined as shown in Fig. 11.

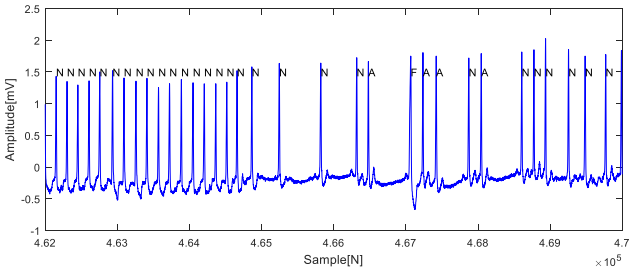

FIGURE 10. Example of RR interval error in Datum of 202.

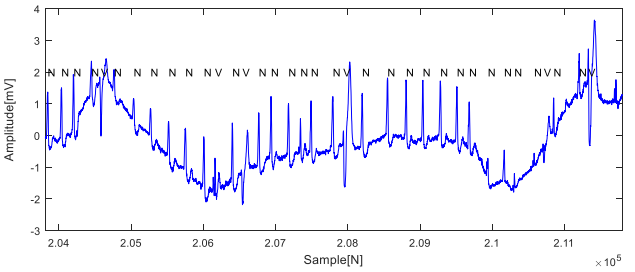

FIGURE 11. Example of baseline error in Datum of 203.

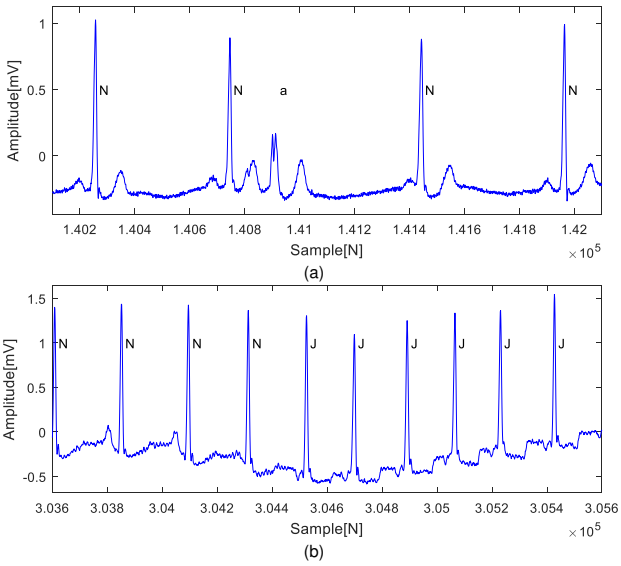

FIGURE 12. Examples of abnormal beats: (a) a, (b) J.

C. FURTHER WORKS

In this paper, we proposed the abnormal beat detection of V, A, F types using shape of waveform and RR interval feature. If we can acquire reliable P-wave features, such as PR interval and P-wave direction, using P-wave's fiducial points, we can expand the algorithm to detect type 'a', aberrated atrial premature beat, and J, junctional premature beat, abnormal beats shown in Table 1. Fig. 12 is the examples of 'a' and J type abnormal beats.

As shown in Fig. 12(a), 'a' type abnormal beat is similar to A or V type abnormal beat. It has short RR interval and small deformation at R-peak. Since the deformation occurs only

TABLE 3. The abnormal beat detection results of MIT-BIH ADB with fixed thresholds, 0.9 in template generation and 0.8 in abnormal beat detection.

Group 1 Record	Normal	Abnormal	TP	TN	FP	FN	Se	Sp	Ac	Group 2 Record	Normal	Abnormal	TP	TN	FP	FN	Se	Sp	Ac
100	2270	34	2236	20	14	0	100.00%	58.82%	99.38%	200	2598	857	1693	817	40	48	97.24%	95.33%	96.61%
101	1860	3	1854	2	1	3	99.84%	66.67%	99.78%	201	1852	230	748	230	0	874	46.12%	100.00%	52.81%
102	2029	4	1995	4	0	30	98.52%	100.00%	98.52%	202	2114	56	1112	55	1	946	54.03%	98.21%	55.20%
103	2081	2	2079	0	2	0	100.00%	0.00%	99.90%	203	2971	445	1954	442	3	572	77.36%	99.33%	80.65%
104	1379	2	1374	1	1	3	99.78%	50.00%	99.71%	205	2653	85	2562	75	10	6	99.77%	88.24%	99.40%
105	2564	41	2461	40	1	62	97.54%	97.56%	97.54%	207	1667	210	1452	198	12	5	99.66%	94.29%	98.98%
106	2024	520	1489	520	0	15	99.00%	100.00%	99.26%	209	3002	384	2617	314	70	1	99.96%	81.77%	97.63%
107	2134	59	2075	57	2	0	100.00%	96.61%	99.91%	210	2624	204	2411	187	17	9	99.63%	91.67%	99.01%
108	1759	23	882	23	0	854	50.81%	100.00%	51.45%	212	1823	0	1823	0	0	0	100.00%	NaN	100.00%
109	2529	40	2480	35	5	9	99.64%	87.50%	99.45%	213	3245	607	2637	61	546	1	99.96%	10.05%	83.14%
111	2121	1	2070	1	0	50	97.64%	100.00%	97.64%	214	2257	257	1971	257	0	29	98.55%	100.00%	98.72%
112	2536	2	2534	1	1	0	100.00%	50.00%	99.96%	215	3360	168	3173	146	22	19	99.40%	86.90%	98.78%
113	1786	0	1768	0	0	18	98.99%	NaN	98.99%	217	1701	162	1538	162	0	1	99.94%	100.00%	99.94%
114	1874	57	1636	57	0	181	90.04%	100.00%	90.34%	219	2151	72	1920	55	17	159	92.35%	76.39%	91.82%
115	1950	0	1950	0	0	0	100.00%	NaN	100.00%	220	2045	94	1949	87	7	2	99.90%	92.55%	99.56%
116	2409	110	2278	109	1	21	99.09%	99.09%	99.09%	221	2424	396	2028	12	384	0	100.00%	3.03%	84.16%
117	1532	1	874	1	0	657	57.09%	100.00%	57.11%	222	2267	208	1437	193	15	622	69.79%	92.79%	71.90%
118	2275	112	2161	60	52	2	99.91%	53.57%	97.63%	223	2585	559	2026	338	221	0	100.00%	60.47%	91.45%
119	1984	443	1538	443	0	3	99.81%	100.00%	99.85%	228	2050	365	1679	347	18	6	99.64%	95.07%	98.83%
121	1860	2	1828	2	0	30	98.39%	100.00%	98.39%	230	2253	1	1936	1	0	316	85.97%	100.00%	85.97%
122	2473	0	2473	0	0	0	100.00%	NaN	100.00%	231	1254	3	1251	2	1	0	100.00%	66.67%	99.92%
123	1515	3	1423	3	0	89	94.11%	100.00%	94.13%	233	3076	848	2225	804	44	3	99.87%	94.81%	98.47%
124	1582	54	1528	44	10	0	100.00%	81.48%	99.37%	234	2700	3	2697	3	0	0	100.00%	100.00%	100.00%
Total	46526	1513	42986	1423	90	2027	95.50%	94.05%	95.45%	Total	54672	6214	44839	4786	1428	3619	92.53%	77.02%	90.77%
										Overall total	101198	7727	87825	6209	1518	5646	93.96%	80.35%	92.92%

TABLE 4. The abnormal beat detection results of MIT-BIH ADB with manually given thresholds for each record.

Group 1 Record	Normal	Abnormal	TP	TN	FP	FN	Se	Sp	Ac	Group 2 Record	Normal	Abnormal	TP	TN	FP	FN	Se	Sp	Ac
100	2270	34	2229	34	0	7	99.69%	100.00%	99.69%	200	2598	857	1717	820	37	24	98.62%	95.68%	97.65%
101	1860	3	1857	2	1	0	100.00%	66.67%	99.95%	201	1852	230	1599	205	25	23	98.58%	89.13%	97.41%
102	2029	4	2025	4	0	0	100.00%	100.00%	100.00%	202	2114	56	1636	54	2	422	79.49%	96.43%	79.94%
103	2081	2	2009	2	0	70	96.63%	100.00%	96.64%	203	2971	445	2401	428	17	125	95.05%	96.18%	95.22%
104	1379	2	1374	2	0	3	99.78%	100.00%	99.78%	205	2653	85	2561	78	7	7	99.73%	91.76%	99.47%
105	2564	41	2523	41	0	0	100.00%	100.00%	100.00%	207	1667	210	1449	210	0	8	99.45%	100.00%	99.52%
106	2024	520	1504	520	0	0	100.00%	100.00%	100.00%	209	3002	384	2577	360	24	41	98.43%	93.75%	97.83%
107	2134	59	2075	59	0	0	100.00%	100.00%	100.00%	210	2624	204	2404	199	5	16	99.34%	97.55%	99.20%
108	1759	23	1704	22	1	32	98.16%	95.65%	98.12%	212	1823	0	1823	0	0	0	100.00%	NaN	100.00%
109	2529	40	2472	38	2	17	99.32%	95.00%	99.25%	213	3245	607	2633	318	289	5	99.81%	52.39%	90.94%
111	2121	1	2117	1	0	3	99.86%	100.00%	99.86%	214	2257	257	2000	257	0	0	100.00%	100.00%	100.00%
112	2536	2	2534	2	0	0	100.00%	100.00%	100.00%	215	3360	168	3158	168	0	34	98.93%	100.00%	98.99%
113	1786	0	1786	0	0	0	100.00%	NaN	100.00%	217	1701	162	1538	162	0	1	99.94%	100.00%	99.94%
114	1874	57	1772	56	1	45	97.52%	98.25%	97.55%	219	2151	72	2078	62	10	1	99.95%	86.11%	99.49%
115	1950	0	1950	0	0	0	100.00%	100.00%	100.00%	220	2045	94	1947	93	1	4	99.79%	98.94%	99.76%
116	2409	110	2299	109	1	0	100.00%	99.09%	99.96%	221	2424	396	2028	396	0	0	100.00%	100.00%	100.00%
117	1532	1	1531	1	0	0	100.00%	100.00%	100.00%	222	2267	208	1498	188	20	561	72.75%	90.38%	74.37%
118	2275	112	2090	109	3	73	96.63%	97.32%	96.66%	223	2585	559	2021	474	85	5	99.75%	84.79%	96.52%
119	1984	443	1541	443	0	0	100.00%	100.00%	100.00%	228	2050	365	1672	365	0	13	99.23%	100.00%	99.37%
121	1860	2	1858	2	0	0	100.00%	100.00%	100.00%	230	2253	1	2252	1	0	0	100.00%	100.00%	100.00%
122	2473	0	2473	0	0	0	100.00%	NaN	100.00%	231	1254	3	1251	2	1	0	100.00%	66.67%	99.92%
123	1515	3	1512	3	0	0	100.00%	100.00%	100.00%	233	3076	848	2225	841	7	3	99.87%	99.17%	99.67%
124	1582	54	1528	52	2	0	100.00%	96.30%	99.87%	234	2700	3	2697	3	0	0	100.00%	100.00%	100.00%
Total	46526	1513	44763	1502	11	250	99.44%	99.27%	99.44%	Total	54672	6214	47165	5684	530	1293	97.33%	91.47%	96.67%
										Overall total	101198	7727	91928	7186	541	1543	98.35%	93.00%	97.94%

around the R-peak, the QRS duration is normal and P-wave is also normally generated. To classify the 'a' type abnormal beat from A or V type abnormal beat, it is important to determine the presence of P-wave. As shown in Fig. 12(b), J type abnormal beat has short PR interval and downward P-wave. So P-wave fiducial points are important to classify the J type abnormal beat.

With various abnormal beat detection, future research aims at detailed abnormal beat classification. Fig. 13 summaries the two steps of further works of this paper.

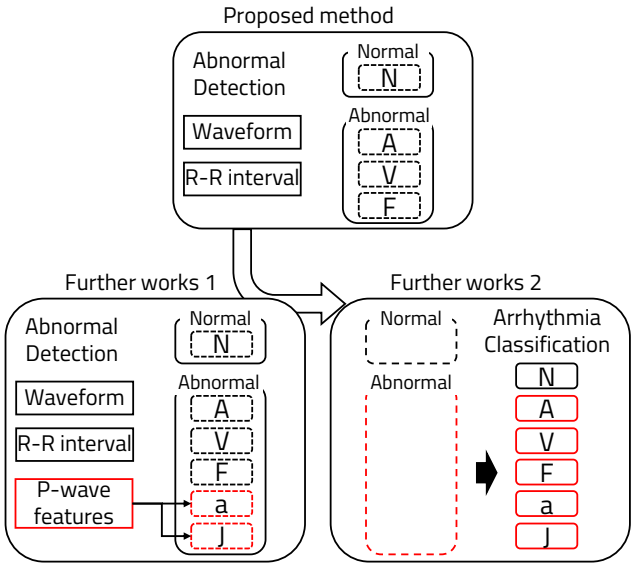

FIGURE 13. Summary of further works.

VI. CONCLUSION

In this paper, we proposed a method for detecting abnormal beats by using feature values and shape together. In particular, during the template cluster generating process, the template was updated using a weighted mean according to the counting number of the template, and a stable normal beat template could be generated through the template cluster. By using RR interval and shape together, it was confirmed that V, A, and F types of abnormal beat can be effectively detected. However, an adaptive determination of a threshold for learning and detection has not been made because the characteristics of beats are different for each individual.

Future experiments could expand to include an automatic detection algorithm for abnormal beat detection through adaptive threshold determination based on the similarity distribution between templates in the template cluster. In addition, the detection of other types of abnormal beats not detected in this paper could be achieved through the refinement of additional feature values or shapes other than the RR interval.

REFERENCES

[1] A. J. Prakash, S. Saunak, and S. Ari, "SpEC: A system for patient specific ECG beat classification using deep residual network," *Biocybernetics and Biomedical Engineering*, vol. 40, no. 4, pp. 1446–1457, 2020.

[2] A. J. Prakash and S. Ari, "A system for automatic cardiac arrhythmia recognition using electrocardiogram signal," *in Bioelectronics and Medical Devices*, Woodhead Publishing, Cambridge, England, 2019, pp. 891–911.

[3] G. S. P. Gomes, and L. H. C. Ferreira, "A lightweight embedded solution for ECG filtering and QRS complexes localization using wavelets," in *2018 IEEE International Symposium on Medical Measurements and Applications*, Rome, Italy, Jun. 2018. pp. 1–6.

[4] B. Mishra, N. Arora, and Y. Vora, "A wearable device for real-time ECG monitoring and cardiovascular arrhythmia detection for resource constrained regions," in *2018 8th International Symposium on Embedded Computing and System Design*, Cochin, India, Dec. 2018. pp. 48–52.

[5] S. Lee, Y. Jeong, J. Kwak, D. Park, and K. H. Park, "Advanced Real-Time Dynamic Programming in the Polygonal Approximation of ECG Signals for a Lightweight Embedded Device," *IEEE Access*, vol. 7, pp. 162850–162861, 2019.

[6] S. Lee, and D. Park, "Enhanced Dynamic Programming for Polygonal Approximation of ECG Signals," in *2020 IEEE 2nd Global Conference on Life Sciences and Technologies*, Kyoto, Japan, Mar. 2020, pp. 121–122.

[7] J. Pan, and W. J. Tompkins, "A real-time QRS detection algorithm," *IEEE Transactions on Biomedical Engineering*, vol. BME-32, no. 3, pp. 230–236, Mar. 1985.

[8] S. Lee, Y. Jeong, D. Park, B.-J. Yun, K. H. Park, "Efficient fiducial point detection of ECG QRS complex based on polygonal approximation," *Sensors*, vol. 18, no. 12, pp. 1–16, Dec. 2018.

[9] A. I. Manriquez, and Q. Zhang, "An algorithm for robust detection of QRS onset and offset in ECG signals," in *2008 Computers in Cardiology*, Bologna, Italy, Sep. 2008, pp. 857–860.

[10] A. I. Manriquez, and Q. Zhang, "An algorithm for QRS onset and offset detection in single lead electrocardiogram records," in *2007 29th Annual International Conference of the IEEE Engineering in Medicine and Biology Society*, Lyon, France, Aug. 2007, pp. 541–544.

[11] J. Dumont, A. I. Hernandez, and G. Carrault, "Parameter optimization of awavelet-based electrocardiogram delineator with an evolutionary algorithm," in *Computers in Cardiology, 2005*, Lyon, France, Sep. 2005, pp. 707–710.

[12] B. S. Raghavendra, D. Bera, A. S. Bopardikar and R. Narayanan, "Cardiac arrhythmia detection using dynamic time warping of ECG beats in e-healthcare systems," in *2011 IEEE International Symposium on a World of Wireless, Mobile and Multimedia Networks*, Lucca, Italy, Jun, 2011, pp. 1–6.

[13] N. Clark, E. Sandor, C. Walden, I. S. Ahn and Y. Lu, "A wearable ECG monitoring system for real-time arrhythmia detection," in *2018 IEEE 61st International Midwest Symposium on Circuits and Systems*, Windsor, ON, Canada, 2018, pp. 787–790.

[14] G. Bansal, P. Gera, and D. R. Bathula, "Template based classification of cardiac arrhythmia in ecg data," in *2015 IEEE 2nd International Conference on Recent Trends in Information Systems*, Kolkata, India, Jul. 2015, pp. 337–341.

[15] R. J. Huszar, *Basic dysrhythmias: interpretation & management.* Mosby Jems/Elsevier, MO, USA, 2007, pp. 1–15.

[16] P. Laguna, R. Jané, and P. Caminal, "Automatic detection of wave boundaries in multilead ECG signals: Validation with the CSE database," *Comput. Biomed. Res.*, vol. 27, no. 1, pp. 45—60, Feb. 1994.

[17] J. Martínez, R. Almeida, S. Olmos, A. Rocha, and P. Laguna, "A wavelet-based ecg delineator: evaluation on standard databases," *IEEE Transactions on Biomedical Engineering*, vol. 51, no. 4, pp. 570–581, Apr. 2004.

[18] J. S. Arteaga-Falconi, H. Al Osman and A. El Saddik, "ECG Authentication for Mobile Devices," *in IEEE Transactions on Instrumentation and Measurement*, vol. 65, no. 3, pp. 591-600, Mar. 2016.

[19] G. B. Moody, and R. G. Mark, "The MIT-BIH arrhythmia database on CD-ROM and software for use with it," in *[1990] Proceedings Computers in Cardiology*, Chicago, IL, USA, Sep. 1990, pp. 185–188.

[20] AAMI, "Testing and Reporting Performance Results of Cardiac Rhythm and ST-segment Measurement Algorithms," *ANSI/AAMI*, Association for the Advancement of Medical Instrumentation and American National Standards Institute, Arlington, VA, USA, 1999.

[21] A. J. Prakash and S. Ari, "AAMI Standard Cardiac Arrhythmia Detection with Random Forest Using Mixed Features," *2019 IEEE 16th India Council International Conference (INDICON)*, Rajkot, India, 2019, pp. 1-4.

[22] M. Merone, P. Soda, and C. Sansone, "ECG databases for biometric systems: A systematic review," *Expert Systems with Applications*, vol. 67, pp. 189–202, Jan. 2017.

[23] F. A. Elhaj, N. Salim, A. R. Harris, T. T. Swee, and T. Ahmed, "Arrhythmia recognition and classification using combined linear and nonlinear features of ECG signals," *Computer Methods and Programs in Biomedicine*, vol. 127, pp. 52–63, Apr. 2016.

[24] G. M. Friesen, T. C. Jannett, M. A. Jadallah, S. L. Yates, S. R. Quint, and H. T. Nagle, "A comparison of the noise sensitivity of nine QRS detection algorithms," *IEEE Transactions on Biomedical Engineering*, vol. 37, pp. 85–98, Jan. 1990.

SEUNGMIN LEE received the B.S. and M.S. degrees in mathematics and the Ph.D. degree in electronics engineering from Kyungpook National University (KNU), Daegu, South Korea, in 2010, 2012, and 2018, respectively. He expanded his research topics to bioinspired signal processing algorithms and electronics systems. He holds BK21 Four Postdoctoral Researcher at School of Electronic and Electrical Engineering in KNU. His research interests include signal processing, image processing, bioinspired signal processing, and compact system implementation. He is focusing his research on the bio-signal processing as the research director of project supported by Basic Science Research Program through the National Research Foundation of Korea (NRF) funded by the Ministry of Education.

DAEJIN PARK received the B.S. degree in electronics engineering from Kyungpook National University, Daegu, Korea in 2001, the M.S. degree and Ph.D. degree in electrical engineering from the Korea Advanced Institute of Science and Technology (KAIST), Daejeon, Korea, in 2003, and 2014, respectively. He was a Research Engineer in SK Hynix Semiconductor, Samsung Electronics over 12 years from 2003 to 2014, respectively and have worked on designing low-power embedded processors architecture and implementing fully AI-integrated system-on-chip with intelligent embedded software on the custom-designed hardware accelerator, especially for hardware/software tightly-coupled applications, such as smart mobile devices, industrial electronics. He was nominated as one of Presidential Research Fellows 21, Republic of Korea in 2014. Prof. Park is now with School of Electronics and Electrical Engineering and School of Electronics Engineering as full-time assistant processor in Kyungpook National University, Daegu, Korea, since 2014. He has published over 180 technical papers and 40 patents.